Exchange Bias as a Probe of the Incommensurate Spin-Density Wave in Epitaxial Fe/Cr(001)

J. S. Parker,[1,2] L. Wang,[1] K. A. Steiner,[1] P. A. Crowell,[2] and C Leighton[1,*]

[1]*Department of Chemical Engineering and Materials Science, University of Minnesota, Minneapolis, Minnesota 55455, USA*
[2]*School of Physics and Astronomy, University of Minnesota, Minneapolis, Minnesota 55455, USA*

(Received 11 July 2006; published 1 December 2006)

We report clear multiple period oscillations in the temperature dependence of exchange bias in an Fe thin film exchange coupled to a neighboring Cr film. The oscillations arise due to an incommensurate spin-density wave in the Cr, with wave vector perpendicular to the Fe/Cr(001) interface. The exchange bias and coercivity allow for a determination of the extent of the thermally driven wavelength expansion, the (strain-suppressed) spin-flip transition temperature, and the Cr Néel temperature, which show a crossover from bulklike to finite-size behavior at a Cr thickness of ~1100 Å. The data are consistent with a transition from a transverse to longitudinal wave on cooling.

DOI: 10.1103/PhysRevLett.97.227206 PACS numbers: 75.30.Fv, 75.70.Cn

Motivated by the discovery of giant magnetoresistance [1,2], the intensive study of Fe/Cr heterostructures has led to the elucidation of much new physics, such as oscillatory coupling [3–6], spin-dependent interfacial scattering [7–9], surface spin flops [10,11], and biquadratic coupling [12,13]. The magnetism of Cr itself has also attracted attention [14]. Bulk Cr orders in an antiferromagnetic (AF) structure known as an incommensurate spin-density wave (ISDW), where the magnitude of the sublattice spin ($\mathbf{S}_{\mathrm{AF}}^{\mathrm{bulk}}$) is sinusoidally modulated [14]. The ISDW has a wave vector $\mathbf{Q}$ and a wavelength $\lambda = 2\pi/|\mathbf{Q}|$ that are incommensurate with the atomic periodicity. Below the Néel temperature (T_N) of 311 K, two phases of the ISDW are found. A high T transverse phase ($\mathbf{Q} \perp \mathbf{S}_{\mathrm{AF}}^{\mathrm{bulk}}$) is separated from a low T longitudinal phase ($\mathbf{Q} \parallel \mathbf{S}_{\mathrm{AF}}^{\mathrm{bulk}}$) by the spin-flip transition temperature $T_{\mathrm{SF}} = 123$ K [14]. Neutron diffraction shows that $\mathbf{Q}$ lies along $\langle 100 \rangle$ and that λ expands with T from 60 Å at 10 K to 78 Å at T_N [14,15]. In thin films, confinement, strain, and proximity to adjacent layers add a new layer of richness. Many differences from bulk are observed, such as coexistence of longitudinal and transverse phases [16], in-plane and out-of-plane $\mathbf{Q}$ and $\mathbf{S}_{\mathrm{AF}}$ [16–22], suppression of T_{SF} [16,18,21,22], and a commensurate SDW [23]. Surprisingly, little has been done to use exchange coupling to probe the Cr spin structure via adjacent Fe layers. It was recently shown that the exchange bias (H_E) at AF/ferromagnet (F) interfaces is influenced significantly by an ISDW in the AF [18]. H_E, a shift of the F's hysteresis loop due to interaction with the AF [24,25], can therefore be used to probe the Cr spin structure.

In this Letter, we report a comprehensive investigation of exchange bias in epitaxial Fe/Cr(001). We observe multiple period oscillations in $H_E(T)$ due to the thermally driven wavelength expansion of an ISDW with $\mathbf{Q}$ perpendicular to the interface. The exchange bias and coercivity (H_C) allow a *quantitative* determination of the extent of the wavelength expansion, the (strain-suppressed) T_{SF}, and the thickness-dependent T_N. The data reveal a crossover from "bulklike" to "finite-size" behavior at a very large thickness (~1100 Å) in addition to allowing us to deduce the relative orientations of $\mathbf{S}_{\mathrm{AF}}$ and $\mathbf{Q}$, both above and below T_{SF}. The results provide further evidence that exchange bias is sensitive to the ISDW and, moreover, that it can be used as a quantitative probe of the complex phenomenology in Cr thin films.

Fe(001)/Cr(001)/Al layers were deposited by dc magnetron sputtering (2×10^{-9} Torr base pressure) on vacuum annealed (500 °C) MgO(001) substrates. 50 Å of Fe was deposited at 0.6 Å s^{-1}, followed by a variable thickness (400 Å $< t_{\mathrm{Cr}} <$ 2100 Å) Cr layer at 0.9 Å s^{-1} and a 30 Å Al capping layer, all at 400 °C and 3 mTorr Ar. Wedged samples were employed in which t_{Cr} was continuously varied (at 19 Å per lateral millimeter) across a single substrate. The constant Fe thickness ensures that the strain state at the F/AF interface is identical for all samples. Structural characterization by wide-angle x-ray diffraction (WAXRD), grazing incidence x-ray reflectivity (GIXR), in-plane diffraction, and atomic force microscopy (AFM) was performed. Prior to measurement, the samples were field cooled in $H_{\mathrm{Cool}} = 350$ Oe, along one of the Fe $\langle 110 \rangle$ directions, from 350 K [increasing the cooling field to as much as 30 kOe produced no changes in the data; an oscillatory $H_E(T)$ and nonmonotonic $H_C(T)$ were still observed]. To measure small oscillations in H_E, magneto-optical Kerr effect measurements were made in a wide-gap Helmholtz coil with a Hall field sensor (absolute and relative field accuracies of 100 and 50 mOe, respectively). SQUID magnetometry was performed in a commercial system with a vector coil set. Figure 1 displays characterization data on a representative sample ($t_{\mathrm{Cr}} = 400$ Å). The WAXRD shows only MgO substrate and Cr(002) peaks, confirming the (001) out-of-plane orientation. The Fe/Cr bilayers grow with the expected epitaxial relationship where the unit cell of the Fe is rotated 45° with respect to that of the MgO. The inset in Fig. 1(a) shows the rocking curve through the Cr(002) peak, which has a width of 0.7°.

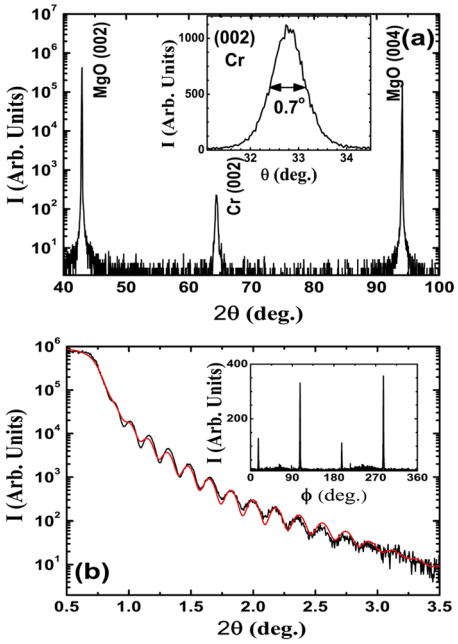

FIG. 1 (color online). (a) Wide-angle x-ray (Cu K_α) diffraction from MgO(001)/Fe(50 Å)/Cr(400 Å)/Al(30 Å). Inset: Rocking curve through Cr (002). (b) Grazing incidence reflectivity. The black line is the data, and the red line is a simulation with a layer thickness (roughness) of 47 (5), 410 (8), and 30 Å (20 Å) for Fe, Cr, and Al, respectively. Inset: In-plane diffraction on Cr (002).

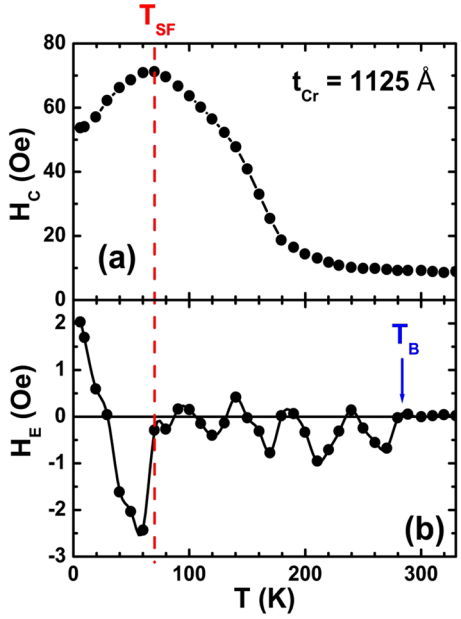

FIG. 2 (color online). Temperature dependence of (a) H_C and (b) H_E for MgO(001)/Fe(50 Å)Cr(1125 Å)/Al(30 Å). T_B (arrow) and T_{SF} (dashed line) are labeled.

The in-plane diffraction (ϕ scan) in the inset in Fig. 1(b) shows four peaks separated by 90°, demonstrating the in-plane epitaxy. The main panel shows the GIXR data, which reveal large amplitude oscillations persisting to 3°. The solid line is a simulation [26] with the layer thicknesses and roughnesses given in the caption. We find an Fe/Cr interfacial roughness of 5 Å, consistent with AFM.

The basic magnetic phenomena are illustrated in Fig. 2, which shows the T dependence of H_E and H_C at $t_{Cr} = 1125$ Å. Examining $H_E(T)$, we observe three distinct regimes. At high T, a blocking temperature (T_B) is visible, above which $H_E = 0$. At intermediate temperatures ($70\ \text{K} < T < 290\ \text{K}$), small but experimentally resolvable oscillations in H_E occur with an amplitude ~1 Oe and period ~40 K. At $T < 70$ K, H_E shows a distinct change in character; the amplitude increases by a factor of 3, but changes in sign still occur. This distinct change in behavior is also evident in H_C. At high temperatures ($T > T_B$), $H_C \sim 10$ Oe, but as T is lowered H_C becomes enhanced, strongly below 200 K, and reaches a peak at 70 K. Several features of the data can be readily interpreted. First, we identify T_B as the actual Néel temperature. This is supported by Fig. 3(b), which shows the t_{Cr} dependence of T_B, as determined from $H_E(T)$, as well as a direct measurement of T_N (measured on samples with constant t_{Cr}) from the well known resistivity anomaly [14]. T_B and T_N coincide at all t_{Cr}. The most unusual aspect of these data, which will be addressed below, is the anomalously large thickness (~1250 Å) at which finite-size effects occur. Note also that prior work found $T_B > 311$ K [23] due to a thin film commensurate SDW phase. The fact that we find T_B values below the bulk T_N implies that the ISDW phase is present. Next, we identify the 70 K transition temperature as T_{SF}. Although $T_{SF} = 123$ K in bulk Cr [14], this is reduced by strain in thin films [16,18,21,22]. Our identification of this temperature as T_{SF} is supported by prior work showing anomalies in H_C at T_{SF} [18,22,27]. T_{SF} is independent of t_{Cr} (within 10 K), presumably due to the fixed strain at the Fe/Cr interface. Finally, in agreement with Yang and Chien [18], we interpret the oscillations in $H_E(T)$ in terms of an ISDW. The oscillations [shown for several thicknesses in Fig. 3(a)] arise due to the T dependence of the ISDW wavelength λ, which is known to expand as $T \rightarrow T_N$, due to weakening of the interatomic exchange. This expansion in λ leads to an oscillation, in both sign and magnitude, of the AF interface moment as it is modulated by the ISDW. The fact that we observe these oscillations implies that (i) $\mathbf{Q}$ is perpendicular to the interface and (ii) the Fe/Cr interface is not a node of the ISDW.

The oscillatory $H_E(T)$ can be quantitatively understood with a simple model. We focus on the region $T > T_{SF}$, where multiple period oscillations occur. A modified Meiklejohn-Bean approach is used [24], i.e., $H_E \propto J_{AF/F}\mathbf{S}_F \cdot \mathbf{S}_{AF}/M_F t_F$, where $J_{AF/F}$ is the interfacial exchange, $\mathbf{S}_F$ is the interfacial Fe moment, M_F and t_F are the saturation magnetization and thickness of the Fe layer, and $\mathbf{S}_{AF}$ is the uncompensated Cr interfacial moment. Ignoring quantities with little or no T dependence, we obtain $H_E \propto \mathbf{S}_{AF}$, where $\mathbf{S}_{AF}$ is modulated by the ISDW. We assume (as confirmed below) that for $T > T_{SF}$, $\mathbf{S}_{AF}$ is in-plane and thus perpendicular to $\mathbf{Q}$. In bulk Cr, the

magnitude of $\mathbf{S}_{AF}$ is proportional to $(1 - T/T_N)^4$ [14], and we model the modulation of $\mathbf{S}_{AF}$ with a sinusoidal function $\sin(t_{Cr}/\lambda(T))$, giving $H_E \propto [(1 - T/T_B)^4 \sin(t_{Cr}/\lambda(T)]$. This assumes that the node of the ISDW occurs at the Cr/Al interface. We assume the same functional form for $\lambda(T)$ as found in bulk [14,15], fix the low T wavelength at the bulk value, and allow the wavelength at T_N to vary. The extent $\Delta\lambda$ of the expansion from $T = 0$ to T_N is therefore an adjustable parameter. The result of fitting to this functional form is shown in Fig. 3(a). Note the increase in oscillation period with decreasing t_{Cr} (as $t_{Cr} \rightarrow \lambda$) and with decreasing T [due to the flattening of $\lambda(T)$ as $T \rightarrow 0$]; i.e., as t_{Cr} increases, the oscillation period decreases and thus more oscillations are observed, as seen in Fig. 3(a). In contrast to Yang and Chien [18], we observe multiple period oscillations where the T and t_{Cr} dependence of the period can be simply understood. The simple model adequately describes the data for all t_{Cr}, with a systematic dependence of $\Delta\lambda$ on t_{Cr}. This is shown in Fig. 3(b), along with the t_{Cr} dependence of T_N. Significantly, the $\Delta\lambda$ for $t_{Cr} > 1000$ Å agrees closely with the known bulk value (18 Å), an important validation of our model. Below this thickness, $\Delta\lambda$ increases rapidly; i.e., both $T_N(t_{Cr})$ and $\Delta\lambda(t_{Cr})$ reveal a clear crossover from bulk to finite-size regimes at low t_{Cr}. The well known features of the ISDW, in particular, the large λ and the acute sensitivity to strain, are consistent with the onset of finite-size effects at large t_{Cr} [16–18,21,22].

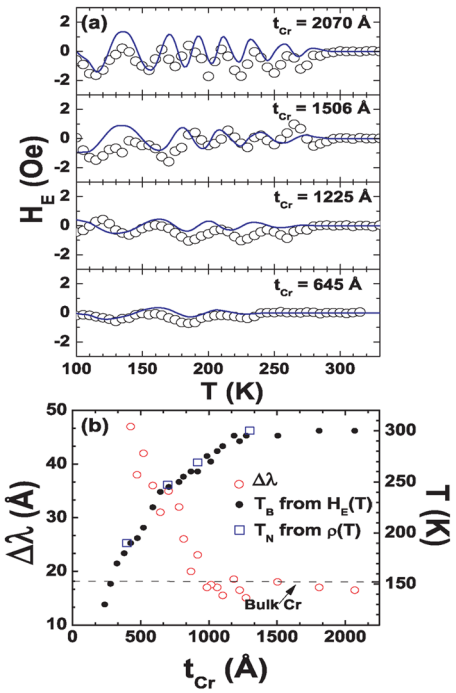

FIG. 3 (color online). (a) Temperature dependence of $H_E(T > T_{SF})$ for MgO(001)/Fe(50 Å)/Cr(t_{Cr})/Al(30 Å) (645 Å $< t_{Cr} <$ 2070 Å). Open points are the data, while lines are fits to the model. (b) t_{Cr} dependence of $\Delta\lambda$ (open red points, left axis) T_B and T_N (right axis). T_B was measured from $H_E(T)$ (solid points) and T_N from $\rho(T)$ (open squares).

In bulk Cr, the spin-flip transition involves reorientation from $\mathbf{S}_{AF}^{bulk} \perp \mathbf{Q}$ (high T) to $\mathbf{S}_{AF}^{bulk} \parallel \mathbf{Q}$ (low T) [14], but thin films and heterostructures are more complex [16–22]. The fact that we consistently observe oscillatory $H_E(T)$ even at $T < T_{SF}$ [Fig. 2(b)] allows us to draw the important conclusion that in our case $\mathbf{Q}$ is always perpendicular to the interface. In order to probe further the orientation of $\mathbf{S}_{AF}$, we used vector magnetometry to assess the exchange anisotropy. The in-plane longitudinal ($\parallel$ to $\mathbf{H}$) and transverse ($\perp$ to $\mathbf{H}$) magnetizations $M_\parallel$ and $M_\perp$ are shown in Fig. 4 for four representative temperatures [320 ($>T_N$), 160 ($T_N > T > T_{SF}$), 100 ($\approx T_{SF}$), and 10 K ($<T_{SF}$)]. The $M_\parallel(H)$ loops are almost T-independent, while $M_\perp(H)$ changes dramatically. The $M(H)$ data were simulated with a coherent rotation model including three anisotropy terms (see the schematic polar plots in Fig. 4): the fourfold anisotropy of the Fe (K_4), the unidirectional exchange anisotropy (K_U), and an exchange-induced uniaxial contribution (K_2). Above T_N, $K_U = K_2 = 0$ (as anticipated), and the simulated and experimental loops [Fig. 4(a)] are in agreement. The abrupt reversal in $M_\perp(H)$ is due to a slight misalignment of $\mathbf{H}$ (by 0.5°) from the hard axis. The field at which this jump occurs decreases rapidly below 200 K [see Figs. 4(c) and 4(e)], and the transverse loop becomes almost closed at 100 K (near T_{SF}). A nonzero K_2 (which turns on at T_N and is therefore exchange-induced) is required to account for this observation. The easy axis of K_2 lies along one of the [100] axes, and its magnitude increases monotonically with decreasing T [Figs. 4(d) and 4(f)], reaching 9×10^4 erg/cm^3 at T_{SF}. Below T_{SF}, the loop reopens dramatically but with $M_\perp(H)$ rotating almost continuously throughout the reversal process [Fig. 4(g)]. As shown in Figs. 4(g) and 4(h), the "reopening" can be approximately modeled by rotating K_2 such that [110] is an easy axis of K_2. Except for the unsurprising overestimation of H_C, the overall agreement with experiment is good.

We propose that, as in bulk Cr, a transverse ISDW occurs above T_{SF}. $\mathbf{Q}$ lies perpendicular to the interface [as required for oscillatory $H_E(T)$], and $\mathbf{S}_{AF}$ is in-plane, consistent with the exchange-induced in-plane uniaxial anisotropy. In bulk, Cr spins orient along the $\langle 100 \rangle$ directions [14]. With $\mathbf{H}_{Cool}$ aligned exactly along [110] [Fig. 4(b)], the alignment of $\mathbf{S}_F$ with $\mathbf{H}_{Cool}$ would lead to equal populations of interface spins along [100] and [010]. In practice, small field misalignment leads to a preference for one of these directions [in Figs. 4(d) and 4(f), it is shown as [010]], giving rise to a uniaxial anisotropy aligned 45° from $\mathbf{H}_{Cool}$, as observed. This anisotropy grows with decreasing T, explaining the strong H_C enhancement below 200 K. At $T < T_{SF}$, the reopening of $M_\perp(H)$ indicates a significant change in the anisotropy. The data can be approximately modeled by a rotation of K_2 such that $\mathbf{H}_{Cool}$ is now an easy axis of K_2 [Fig. 4(h)]. This is difficult to explain while maintaining in-plane $\mathbf{S}_{AF}$ (due to

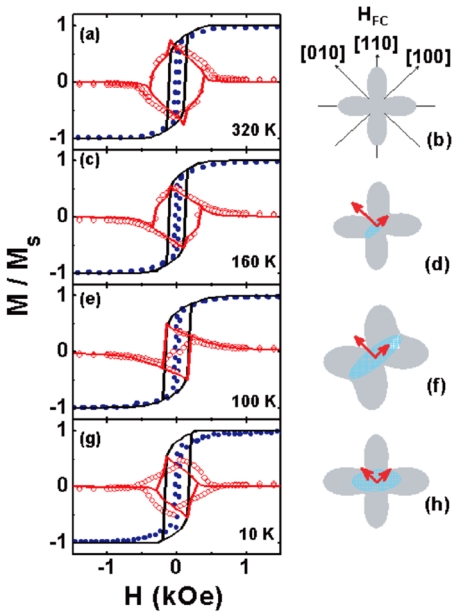

FIG. 4 (color online). Longitudinal (solid blue circles) and transverse (open red circles) $M(H)$ loops at $T =$ (a) 320, (c) 160, (e) 100, and (g) 10 K for MgO(001)/Fe(50 Å)/Cr(1500 Å)/Al(30 Å). The solid lines are simulations for the longitudinal (black) and transverse (red) situations. The model parameters at 320, 160, 100, and 10 K are $K_4 = 3.2 \times 10^5$ erg/cm^3, $K_2 = 0$; $K_4 = 3.2 \times 10^5$ erg/cm^3, $K_2 = 2.1 \times 10^4$ erg/cm^3, $\phi = 45°$; $K_4 = 3.2 \times 10^5$ erg/cm^3, $K_2 = 9.0 \times 10^4$ erg/cm^3, $\phi = 45°$; and $K_4 = 3.2 \times 10^5$ erg/cm^3, $K_2 = 9.0 \times 10^4$ erg/cm^3, $\phi = 0°$, respectively, where ϕ is the angle between H_{Cool} and the uniaxial anisotropy. The right panels show corresponding schematic polar plots of the total energy surface (gray), K_2 (cyan hatched region), and $\mathbf{S}_{\text{AF}}$ [out of plane in (h)].

preferred orientations along the ⟨100⟩ directions) but it can be simply explained if $\mathbf{S}_{\text{AF}}$ is oriented out-of-plane. The cooling field (and alignment of $\mathbf{S}_F$) induces canting of the out-of-plane AF spins, resulting in an easy axis along $\mathbf{H}_{\text{Cool}}$. These data are therefore consistent with a longitudinal ISDW for $T < T_{\text{SF}}$, as is observed in bulk. Although the distinct change in character in $H_E(T)$ at $T < T_{\text{SF}}$ [Fig. 2(b)] is explained by this model, the increase in magnitude is more difficult to understand. Recent work on Cr crystals using spin-polarized scanning tunneling microscopy has revealed that the longitudinal ISDW does not extend to the surface, leading to a domain wall in the subsurface region [28]. This would explain the dramatic change in H_E and the anisotropy surface below 100 K. The complexity of the actual anisotropy in this situation is likely responsible for the significant discrepancies between the experimental data and our simple rotation model for $T < T_{\text{SF}}$.

In summary, we have presented a comprehensive investigation of the incommensurate spin-density wave ordering in thin film Cr using exchange coupling to adjacent Fe layers. Distinct oscillations in the exchange bias are understood within a simple model, enabling extraction of the Cr Néel temperature, the spin-flip transition temperature, and the extent of the thermally driven wavelength expansion. A clear crossover from bulk to finite-size behavior is observed at large thickness, highlighting the sensitivity to strain and the presence of interfaces. The nature of the exchange bias and induced anisotropy allows us to deduce the relative orientations of the AF spins and the propagation direction of the spin-density wave.

This work was supported primarily by the MRSEC program of the NSF under Grant No. DMR 02-12302.

*Electronic address: leighton@umn.edu

[1] M. N. Baibich *et al.*, Phys. Rev. Lett. **61**, 2472 (1988).
[2] P. Grünberg *et al.*, Phys. Rev. Lett. **57**, 2442 (1986).
[3] S. S. P. Parkin, N. More, and K. P. Roche, Phys. Rev. Lett. **64**, 2304 (1990).
[4] S. S. P. Parkin, Phys. Rev. Lett. **67**, 3598 (1991).
[5] J. Unguris, R. J. Celotta, and D. T. Pierce, Phys. Rev. Lett. **67**, 140 (1991).
[6] C. D. Potter *et al.*, Phys. Rev. B **49**, 16 055 (1994).
[7] E. E. Fullerton *et al.*, Phys. Rev. Lett. **68**, 859 (1992).
[8] R. Schad *et al.*, Europhys. Lett. **44**, 379 (1998).
[9] J. Santamaria *et al.*, Phys. Rev. B **65**, 012412 (2001).
[10] R. W. Wang *et al.*, Phys. Rev. Lett. **72**, 920 (1994).
[11] S. G. E. te Velthuis, J. S. Jiang, S. D. Bader, and G. P. Felcher, Phys. Rev. Lett. **89**, 127203 (2002).
[12] M. Rührig *et al.*, Phys. Status Solidi A **125**, 635 (1991).
[13] J. Meersschaut, C. L'abbé, M. Rots, and S. D. Bader, Phys. Rev. Lett. **87**, 107201 (2001).
[14] E. Fawcett, Rev. Mod. Phys. **60**, 209 (1988).
[15] S. A. Werner, A. Arrott, and H. Kendrick, Phys. Rev. **155**, 528 (1967).
[16] P. Bödeker, A. Schreyer, and H. Zabel, Phys. Rev. B **59**, 9408 (1999); P. Bödeker *et al.*, Phys. Rev. Lett. **81**, 914 (1998).
[17] E. E. Fullerton, S. D. Bader, and J. L. Robertson, Phys. Rev. Lett. **77**, 1382 (1996).
[18] F. Y. Yang and C. L. Chien, Phys. Rev. Lett. **90**, 147201 (2003).
[19] K. Mibu *et al.*, Phys. Rev. Lett. **89**, 287202 (2002).
[20] E. E. Fullerton *et al.*, Phys. Rev. Lett. **91**, 237201 (2003).
[21] J. E. Mattson, S. D. Bader, M. B. Brodsky, and J. B. Ketterson, J. Magn. Magn. Mater. **109**, 179 (1992).
[22] J. Pflaum *et al.*, IEEE Trans. Magn. **34**, 1036 (1998); J. Pflaum *et al.*, J. Magn. Magn. Mater. **198**, 453 (1999).
[23] F. Y. Yang and C. L. Chien, J. Appl. Phys. **93**, 6829 (2003).
[24] J. Nogués and I. K. Schuller, J. Magn. Magn. Mater. **192**, 203 (1999).
[25] W. H. Meiklejohn, Phys. Rev. **105**, 904 (1957).
[26] PANalytical B.V. X'PERT REFLECTIVITY software package, v 1.0.
[27] A. Berger and H. Hopster, Phys. Rev. Lett. **73**, 193 (1994).
[28] T. Hänke *et al.*, Phys. Rev. B **71**, 184407 (2005).